Journal of Molecular Catalysis A: Chemical 302 (2009) 86–96

Contents lists available at ScienceDirect

Journal of Molecular Catalysis A: Chemical

journal homepage: www.elsevier.com/locate/molcata

$Ag–Al_2O_3$ catalysts for lean NO_x reduction—Influence of preparation method and reductant

Hannes Kannisto*, Hanna Härelind Ingelsten, Magnus Skoglundh

Competence Centre for Catalysis (KCK), Department of Chemical and Biological Engineering, Chalmers University of Technology, SE-412 96 Göteborg, Sweden

ARTICLE INFO

Article history:
Received 29 August 2008
Received in revised form
28 November 2008
Accepted 1 December 2008
Available online 6 December 2008

Keywords:
Lean NO_x reduction
Ag
Al_2O_3
Impregnation
Sol–gel

ABSTRACT

Alumina supported silver catalysts for selective catalytic reduction of NO_x with hydrocarbons under excess oxygen (HC-SCR) were prepared according to three different methods. These are impregnation (I) and two different sol–gel routes, via thermal drying (II) or freeze-drying (III). The latter method has not previously been reported for preparation of $Ag–Al_2O_3$ catalysts. The prepared samples were characterized by N_2-sorption, TEM, XRD and XPS, and the catalytic properties were further investigated in flow reactor experiments. Two different hydrocarbons (propene and *n*-octane) were used separately as reductants for the SCR reaction. The TEM, XRD and XPS analyses confirmed that the sol–gel samples contain more dispersed silver of higher oxidation state than the corresponding impregnated sample. Further, it was shown that the freeze-dried sol–gel samples most likely contain well dispersed silver throughout the alumina matrix, mainly as oxidized silver. The XPS results also strongly indicate the presence of silver clusters on the surface of samples prepared by routes (I) and (II). The results from the flow reactor study imply that the ratio between silver clusters and oxidized silver species is crucial to achieve high NO_x reduction.

1. Introduction

Global warming is pointed out as one of the most important environmental threats in modern time. The awareness of the relation between global warming and anthropogenic emissions of carbon dioxide has rapidly increased after the release of the 1st 2007 IPCC environmental report [1] in February 2007. To meet the requirements for lower CO_2 emissions, combustion systems that operate at high excess of oxygen such as lean burn and diesel engines, can be used, but this calls for development of more efficient NO_x abatement techniques. Among other techniques, selective catalytic reduction of NO_x with hydrocarbons (fuels) as reducing agent (HC-SCR) is a convenient technique, which offers advantages concerning e.g. distribution of the reducing agent.

A promising catalyst for HC-SCR is silver-alumina [2–8], over which high conversion of NO_x to N_2 with hydrocarbons as reductant has been demonstrated [4,6,9–14]. The most significant drawback of the silver-alumina system is the rather high temperatures required to activate the hydrocarbons [3–5,8,15]. However, by using long-chained hydrocarbons the SCR reaction has previously been shown to proceed at lower temperatures and with broader activity window, compared to using shorter hydrocarbons [12,14,16]. The reason for this effect is suggested to be related to the lower activation (i.e. partial oxidation) temperature for longer hydrocarbons, compared to shorter [12,17]. Also, the addition of low amounts of hydrogen has shown remarkable effects on the SCR activity at even lower temperatures [18,19].

Several studies show that the catalytic properties of silver-alumina are strongly dependent on the silver loading [5,14,16,20], where around 2 wt.% Ag is reported to be the optimal loading for impregnated catalysts. Most commonly, γ-alumina is used as the support material for silver, but other types of alumina supports have also been reported [16,21,22]. The state of silver has been thoroughly discussed [14,23–29], and the active phase is suggested to be small clusters of ionic silver ($Ag_n^{\delta+}$) [26,28,29], Ag^+ ions [14,23], Ag–O–Al species [25] or a combination of these. Recently, Hellman and Grönbeck [27] suggested that the alumina is activated for NO_2 adsorption in the proximity of small silver clusters. A high ratio of these non-metallic silver species seems to give a highly active catalyst for selective reduction of NO_x to N_2 under lean conditions. Higher amounts of metallic silver promote oxidation reactions [4,8,14,20,23,25,30], which results in combustion of the reducing agent.

The objective of the present study is to compare three different preparation methods for silver-alumina catalysts with respect to catalytic activity and selectivity for lean NO_x reduction, using propene or *n*-octane as the reducing agent. The preparation methods compared in this study are impregnation, based on the method

* Corresponding author. Tel.: +46 31 772 3372; fax: +46 31 160062.
E-mail address: hannes.kannisto@chalmers.se (H. Kannisto).

1381-1169/$ – see front matter © 2008 Elsevier B.V. All rights reserved.
doi:10.1016/j.molcata.2008.12.003

described by Iglesiaz-Juez et al. [24], a sol–gel method based on the preparation route presented by Seker et al. [31] and a new sol–gel route presented in this report, including freeze-drying of the formed gel. The activity and selectivity of the prepared samples have been analyzed using a continuous flow reactor. These results are discussed in relation to differences in other characteristics, such as BET surface area, pore-size distribution and chemical state of the silver in both bulk and surface of the catalysts. Also, XPS is proposed as a tool for detecting silver clusters on the surface of silver alumina catalysts.

2. Experimental

2.1. Catalyst preparation

Silver-alumina catalysts are commonly prepared by impregnation of the alumina support with silver [4,21,24]. The pre-prepared alumina powder is exposed to a solution of a silver precursor, with or without addition of a complex agent to remove the charge repulsive forces between silver ions and the alumina surface [24]. The optimum loading of silver for this method is reported to be around 2 wt.% [5,14,16,20]. Another way of preparation is by a sol–gel method [12,14,31], where an aluminium hydroxide sol is prepared and subsequently mixed with a solution of the silver precursor. As the solvent is removed a gel containing both silver and aluminium hydroxide is formed. The gel is dried, usually ground and finally calcined and the resulting catalyst is composed of an alumina substrate with silver evenly distributed throughout the material.

Fig. 1 describes the preparation methods used in this study. The samples prepared are designated by an abbreviation indicating the preparation technique (IM: impregnation, SG: thermally dried sol–gel, F: freeze-dried sol–gel), followed by a number indicating the nominal silver content in the sample.

2.1.1. Preparation route I: impregnation

Silver-alumina catalysts with different silver loading were prepared according to the method described by Iglesias-Juez et al. [24]. Aqueous solutions of $AgNO_3$ (>99.5%; VWR) were mixed with EDTA (≥99.4%; Sigma–Aldrich) and the pH was adjusted to 6.3 with addition of tetramethylammonium hydroxide (TMAH, 10–25%; Merck), to obtain negatively charged silver complexes. The amount of Ag–EDTA solution corresponding to the nominal silver content of the final catalyst was then added to an aqueous slurry of the alumina support (Puralox SBa 200; SASOL), which was subsequently stirred for 2 h. The pH was adjusted to 6.3 by addition of HNO_3 (15%; Fluka). The slurry was then freeze-dried and the resulting powder was heated in air at a rate of 2 °C/min to 600 °C and finally calcined at constant temperature for 6 h.

2.1.2. Preparation route II: thermally dried sol–gel

Using this procedure, the silver-alumina samples were prepared according to a single step sol–gel method presented by Seker et al. [31]. Aluminium isopropoxide (98+%; Aldrich) and a small quantity of 65% HNO_3 (Fluka) in the ratio of 0.195 mol HNO_3/mol AIP, were mixed in water (milli-Q; 10 ml water/g AIP) to form an aluminium hydroxide sol. Silver nitrate (>99.5%; VWR) corresponding to the nominal silver loading of the final catalyst was dissolved in water (milli-Q) and added to the sol, which was stirred for 12 h. The solvent was thereafter removed under reduced pressure at 50 °C, to form a gel. The gel was subsequently dried in air at 100 °C and

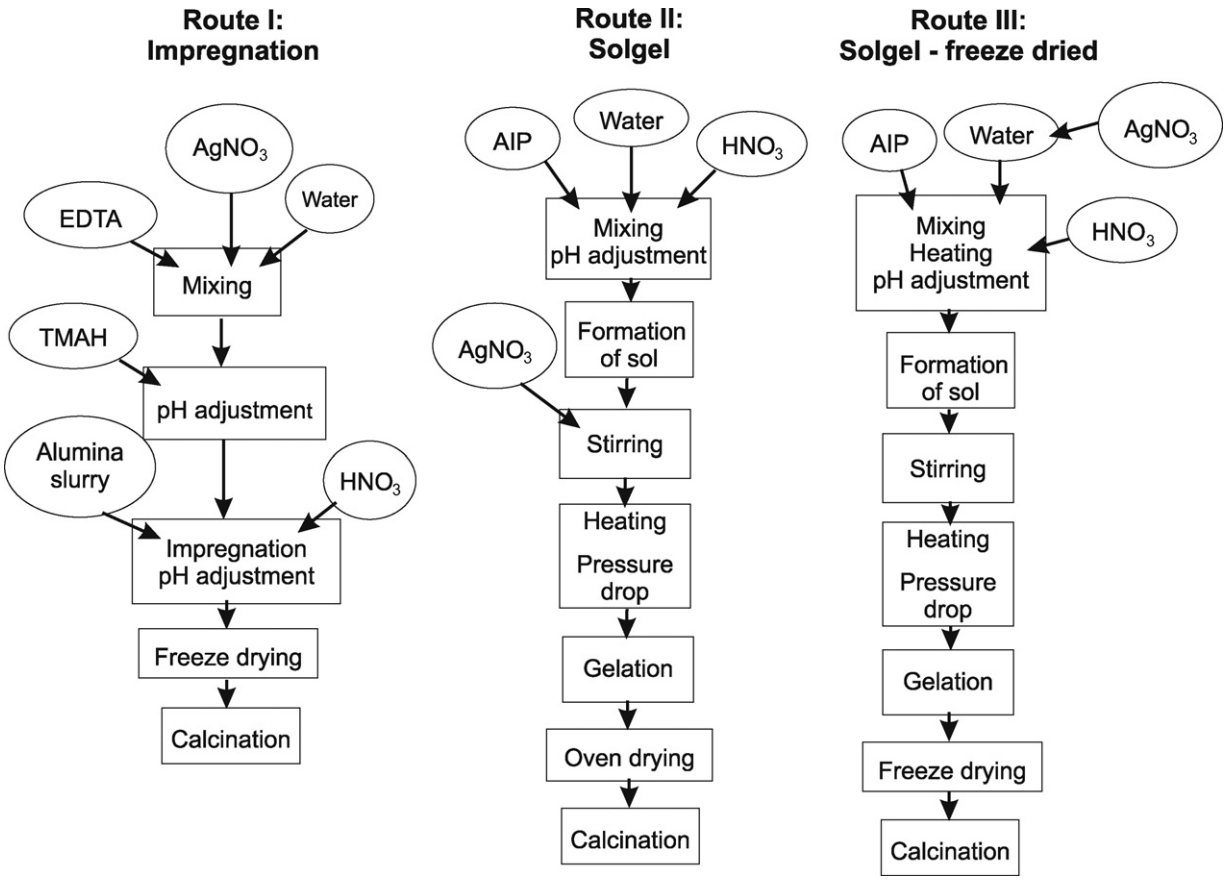

Fig. 1. Preparation routes for the silver alumina catalysts.

crushed to a fine powder. The resulting powder was heated in air at a rate of 2 °C/min to 600 °C and finally calcined at constant temperature for 6 h.

2.1.3. Preparation route III: freeze-dried sol–gel

Silver nitrate (>99.5%; VWR) was dissolved in water (milli-Q) and aluminium isopropoxide (98+%; Aldrich) was slowly added to the $AgNO_3$ solution under vigorous stirring. The $AgNO_3$/AIP/water ratio was similar as in Route II. The resulting slurry was heated to 80 °C and nitric acid (10%; Fluka) was subsequently added dropwise until the slurry cleared, i.e. a sol was formed. The sol was kept under stirring for 12 h. Excess solvent was removed under reduced pressure at 45 °C until a gel formed. The gel was freeze-dried and crushed to a fine powder, which was heated in air by 2 °C/min to 600 °C and finally calcined at constant temperature for 6 h.

2.1.4. Coating of monolith substrates

Corderite monoliths (400 CPSI, 188 channels) were cut from a 20 mm thick block and then calcined in air at 600 °C for 3 h. The silver-alumina powder was mixed with boehmite (Disperal Sol P2; Condea) in a weight ratio of 4:1 and then added to water (milli-Q) under vigorous stirring, forming a slurry containing 20% dry material. The monolith was coated by immersion in the slurry. Excess slurry was removed from the channels by gently blowing air through the channels. The coated monolith was then dried in a 90 °C air stream for ca 15 min and subsequently calcined in hot air (∼500 °C) for 5 min. The procedure was repeated until catalytic material corresponding to 20% of the total weight was deposited on the coated monolith. The monolith was finally calcined in air for 3 h at 600 °C. The monoliths were designated according to the corresponding catalyst in the washcoat.

2.2. Characterization

All samples were characterized by N_2 sorption, while selected samples prepared by each route were further characterized by X-ray diffraction (XRD), X-ray photoelectron spectroscopy (XPS) and transmission electron microscopy (TEM). Powders from the prepared samples have been sieved, showing a particle size distribution of 78% <90 μm and 58% <45 μm for the sol–gel samples. The alumina used for impregnation (SBa200, Sasol) showed a particle size distribution of 96% <90 μm and 71% <45 μm.

2.2.1. N_2 sorption

The specific surface area and the pore-size distribution of the samples, before coating onto monoliths, were determined by N_2 sorption at 77 K using a Micromeritics TriStar instrument, according to the BET [32] and BJH [33] method, respectively. All samples were dried at 200 °C in vacuum for 2 h before analysis.

2.2.2. XRD

X-ray diffraction was used to determine the bulk composition of the selected samples and to give an indication of the relative particle sizes between these samples. The instrument used was a Siemens D5000 X-ray diffractometer with Bragg-Brentano geometry and a Cu Kα source.

2.2.3. XPS

X-ray photoelectron spectroscopy studies were performed to determine the surface composition of the selected samples. The instrument used was a Perkin-Elmer PHI 5000C system equipped with a pre-treatment reactor cell. The system has previously been described in detail in [34].

The catalyst samples were coated onto cordierite monoliths and then placed on the same sample holder, together with a silicon wafer covered by 10 nm of titanium, subsequently covered by a 200 nm thick silver layer. The XPS analyses were performed after pre-treatment at 400 °C for 10 min in 5% oxygen or 4% hydrogen flow (300 ml/min, Ar bal.), respectively. The samples were cooled to 100 °C in the respective gas flow and further cooled to room temperature in vacuum, before transfer to the UHV chamber. The XPS spectra were obtained using monochromatic Mg Kα radiation and the Ag $3d_{5/2}$, Al 2s, O 1s and C 1s core levels were thoroughly studied. As charging of the material was evident, correction was made by shifting the spectra, using the C 1s peak at 284.5 eV [35] as reference. The shift between the C 1s and the Al 2s peaks was also checked to be constant for all samples, to ensure a valid correction. Deconvolution of the Ag $3d_{5/2}$ peaks was performed by fitting a sum of three Gaussian peaks to the Ag $3d_{5/2}$ peak of the different samples. These Gaussian functions were forced to peak at the binding energies of Ag^{2+}, Ag^{+} and Ag^{0} according to [35], respectively, with an allowed deviation of ±0.1 eV. To ensure a valid fit, the r^2 value was compared to the corresponding value of unrestricted fittings of sums of two and three Gaussian peaks, respectively. The difference between those r^2 values was less than 1% for all cases.

2.2.4. TEM

Transmission electron microscopy images of the selected samples were obtained to give an indication of the silver particle size and the dispersion of the silver. The instrument used was a JEOL JEM-1200 EX II. Sample grids (Cu, 3.0 mm, 300 mesh) were prepared by placing a drop of finely ground sample powder dispersed in ethanol onto the grid and excess solvent was finally removed.

2.3. In situ DRIFTS experiments

In order to characterize the OH-groups on the sample surface, *in situ* FTIR (Fourier Transform Infrared) spectroscopy measurements were carried out using a BioRad FTS 6000 spectrometer equipped with a Harrick Praying Mantis DRIFT (diffuse reflection infrared Fourier transform) reaction cell [36,37]. The samples were initially pre-treated in oxygen (8% O_2 in Ar, 500 °C, 30 min) and then evacuated in pure Ar (500 °C, 15 min) at a total flow rate of 150 ml/min. Background spectra (50 scans at a resolution of 1 cm^{-1}) were collected under Ar exposure at 450 °C.

2.4. Flow reactor experiments

The flow reactor system used for evaluation of the catalytic performance of the samples has been described in detail previously [38,39]. The reactor consisted of a horizontal quartz tube heated by a heating coil, where the temperature was measured by two thermocouples (type K), 15 mm before the sample and inside the monolith sample (just before the rear end), respectively. The inlet gas composition was controlled by an Environics 2000 gas mixer. In all experiments, the inlet gas mixture was composed of 500 ppm NO, 1500 ppm C_1 (in form of propene or octane) and 5% O_2, with argon as carrier gas. The total flow was 3500 ml/min, which corresponds to GHSV 30,000 h^{-1}. The reactor outlet gas composition was analyzed with respect to total NO_x, NO and NO_2 by a MKS 2000 FTIR instrument and a 700 EL ht chemiluminescense NO_x detector (Eco Physics). The N_2O content was analyzed by the MKS 2000 FTIR instrument and the CO_2 content was measured by an UNOR 610 non-dispersive IR CO_2 analyzer (Maihak). The analysis was performed during both heating and cooling ramps of 5 °C/min between 250 and 550 °C. Prior to each experiment the samples were pre-treated in 8% O_2 (Ar bal.) at 550 °C for 20 min. Octane was introduced to the reactor via an external CEM-system (controlled evaporator mixer; Bronkhorst), where the octane and carrier gas flows were controlled by mass flow controllers and then mixed at constant temperature (25 °C).

Data from the flow reactor experiments were analyzed with respect to NO_x reduction and N_2O formation for all samples. For the sample showing the highest NO_x reduction with octane as reductant and the corresponding samples prepared by the other preparation routes, the data were further analyzed with respect to CO_2 and NO_2 formation, both for propene and *n*-octane as reductant.

The samples were calcined in air at 600 °C for 6 h and additionally after coating onto the monolith substrates for another 3 h, prior to the reactor studies. During the experiments, the temperature did not exceed 550 °C. Previously, Kylhammar et al. [40] showed that Ag/Al_2O_3 is stable in respect to NO_x reduction for calcination temperatures up to 850 °C. Decrease in NO_x reduction was not observed until the calcination temperature reached 950 °C. Therefore, the samples in this work are most likely stable during the reactor study.

3. Results and discussion

3.1. Catalytic performance

The results from the NO_x reduction experiments with propene as reductant are summarized in Table 1 and Fig. 2, showing the results of the heating ramps. Fig. 2a shows the NO_x reduction as function of the catalyst inlet temperature for the samples with 2 wt.% nominal silver loading, prepared according to the three preparation routes; impregnation (IM), thermally dried sol–gel (SG) and freeze-dried sol–gel (F). Comparing the maximum NO_x reduction, the SG2 sample shows the lowest maximum of 22% with the corresponding temperature at 527 °C. The IM2 and F2 samples show considerably higher NO_x reduction (59% at 513 °C and 58% at 539 °C, respectively). All samples show quite narrow NO_x reduction temperature windows. No significant NO_x reduction is shown below 400 °C for any sample, while the maxima in NO_x reduction are reached in the temperature interval 510–540 °C. Fig. 2b and c show the NO_x reduction over the samples with 5 and 8 wt.% nominal silver loading, respectively. In general, increased silver loading lowers the temperature for maximum NO_x reduction and broadens the NO_x reduction temperature window for all samples. It is notable that the freeze-dried sol–gel samples show very similar maxima in NO_x reduction, regardless of silver loading. However, the SG8 sample does not follow the general trend (Fig. 2c), as the temperature for maximum NO_x reduction is higher compared to the SG5 sample, although the NO_x reduction temperature window is broader. The lowest NO_x reduction is shown for the IM8 sample (14% at 453 °C). However, at temperatures below 350 °C this sample demonstrates significantly higher NO_x reduction (approximately 10%) than any other sample.

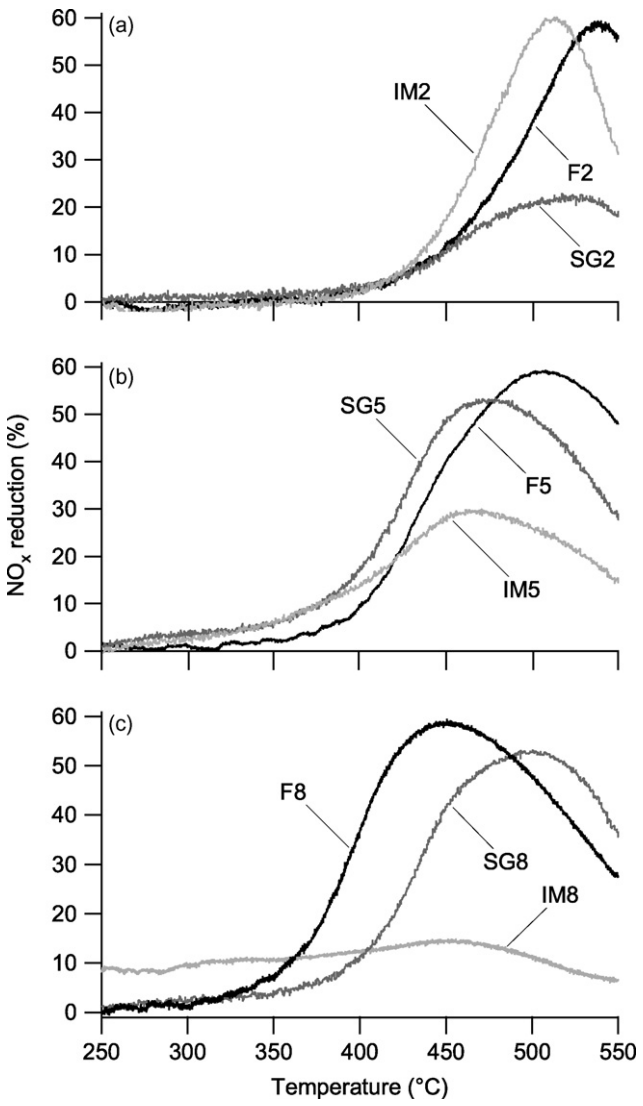

Fig. 2. Reduction of NO_x with propene as reductant for samples with nominal Ag content of 2 wt.% (a), 5 wt.% (b) and 8 wt.% (c). The samples are prepared via the impregnation (IM), thermally dried sol–gel (SG) and freeze-dried sol–gel (F) routes. Number index refers to the nominal silver content in the catalyst. Inlet gas flow composition: 500 ppm NO, 500 ppm C_3H_6 (1500 ppm HC_1), 5% O_2, Ar bal. GHSV: 30,000 h^{-1}. Temperature measured 15 mm before the monolith sample.

Table 1 and Fig. 3 summarize the results from the heating ramps of the NO_x reduction experiments with *n*-octane as reductant. Fig. 3a shows the NO_x reduction vs. temperature for the samples with 2 wt.% silver loading. As for propene as reductant (Fig. 2a), the SG2 sample shows the lowest NO_x reduction (26%), while the IM2 and F2 samples show significantly higher NO_x reduction (45% and 47%, respectively). The NO_x reduction temperature window is significantly broader compared to propene as reductant, but

Table 1
Maximum NO_x reduction with corresponding temperature and Weiszs-modulus at 475 °C for the $Ag–Al_2O_3$ samples.

Sample	Reductant					
	Propene			Octane		
	Max NO_x reduction (%)	Corresponding temperature (°C)	Weiszs-modulus	Max NO_x reduction (%)	Corresponding temperature (°C)	Weiszs-modulus
IM2	59	513	0.65	45	517	0.56
SG2	22	527	0.28	26	544	0.24
F2	58	539	0.37	47	533	0.48
IM5	29	469	0.56	26	354	0.19
SG5	53	474	0.99	52	404	0.45
F5	59	508	0.99	35	487	0.61
IM8	14	453	0.28	24	436	0.39
SG8	53	502	0.93	32	347	0.20
F8	58	452	1.02	31	453	0.56

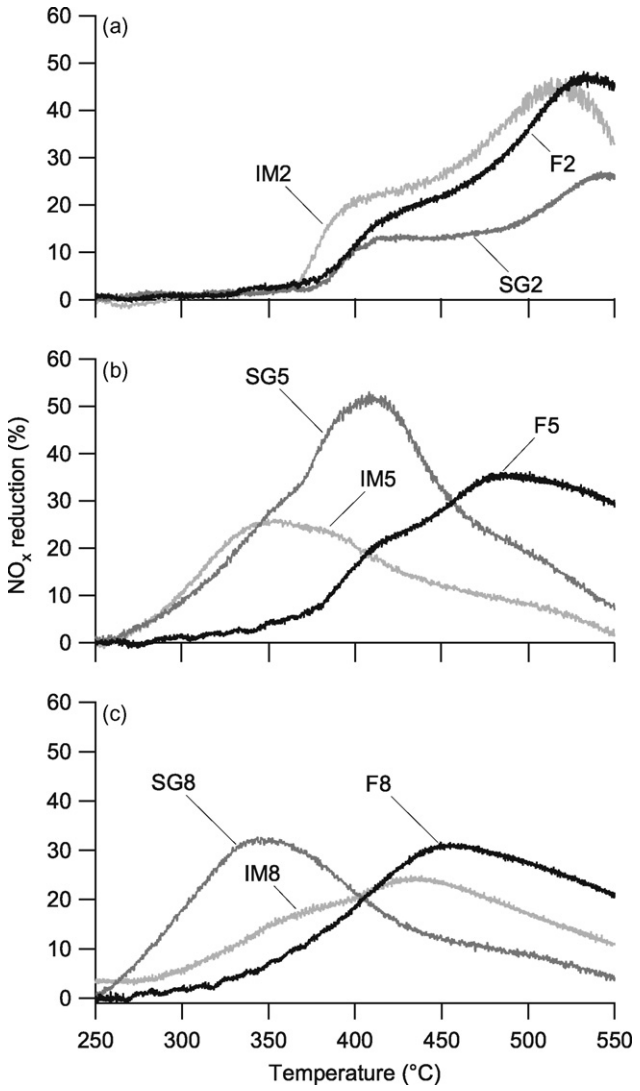

Fig. 3. Reduction of NO_x with octane as reductant for samples with nominal Ag content of 2 wt.% (a), 5 wt.% (b) and 8 wt.% (c). The samples are prepared via the impregnation (IM), thermally dried sol–gel (SG) and freeze-dried sol–gel (F) routes. Number index refers to the nominal silver content in the catalyst. Inlet gas flow composition: 500 ppm NO, 188 ppm C_8H_{18} (1500 ppm HC_1), 5% O_2, Ar bal. GHSV: 30,000 h^{-1}. Temperature measured 15 mm before the monolith sample.

the maximum NO_x reduction is reached in a similar temperature interval (515–545 °C) as for propene, for all samples with 2 wt.% nominal silver loading. Contrary as for propene, the NO_x reduction with octane does not increase smoothly with temperature. Instead, there is a plateau in the NO_x reduction in the temperature interval 400–460 °C. The results for the samples with 5 and 8 wt.% silver content are presented in Fig. 3b and c, respectively. The general trend is similar as for propene as reductant, i.e. increased silver loading results in lower temperature for the maximum NO_x reduction and a broader temperature window. In contrast to propene as reductant, the SG samples follow this trend. However, the IM8 sample shows a higher temperature for maximum NO_x reduction (Fig. 3c), compared to the IM5 sample (Fig. 3b). Further, most samples show lower maximum NO_x reduction with octane, compared to propene. The IM8 sample is an exception, increasing the maximum NO_x reduction. The SG5 sample (Fig. 3b) shows the highest NO_x reduction of all samples, virtually the same maximum NO_x reduction as with propene as reductant, although the corresponding temperature is lower. This decrease in temperature for maximum NO_x reduction for octane as reducing agent is noticed for most samples with 5 or 8 wt.% nominal silver loading, most significant for the SG5 and SG8 samples. However, the samples with 2 wt.% silver loading (Fig. 3a) show maximum NO_x reduction at similar temperatures (IM2 and F2 samples), or at higher temperature (SG2 sample). The F8 sample also shows maximum NO_x reduction at a similar temperature with octane as reducing agent, compared to propene. The amount of formed N_2O never exceeds 8 ppm (less than 2% of total NO_x) for any sample, regardless of reducing agent (not shown).

Table 2
Ignition temperature, i.e. temperature for CO_2 formation corresponding to 50% conversion of the hydrocarbon [42,43], for samples with 5 wt.% nominal silver loading.

Sample	Reductant	
	Propene	Octane
	Ignition temperature [°C]	
IM5	404	329
SG5	427	388
F5	464	432

In order to investigate if the catalytic activity was limited by mass transport of reactants, the Weiszs-modulus [41] was estimated for each sample by

$$\Phi = \frac{L^2 r}{D_{eff} c_{as}} \quad (1)$$

where L is the thickness of the washcoat layer, r the reaction rate, D_{eff} the effective diffusivity and c_{as} the surface concentration of the reactant. $\Phi \geq 1$ indicates mass transport limitations for the reactant. The estimation was made at 475 °C with NO as the reactant. The results are summarized in Table 1. It is apparent that mass transport limitation may be an issue for the IM5, F5 and F8 samples, with propene as reductant. For *n*-octane however, mass transport limitations can be neglected.

Further analysis of the flow reactor data was performed for the samples with 5 wt.% silver loading, as the SG5 sample showed the highest NO_x reduction with octane as reductant. The results are summarized in Table 2, Figs. 4 and 5. Fig. 4a shows the total CO_2 formation and the CO_2 formation due to combustion of the reductant as function of temperature over the selected samples (i.e. IM5, SG5 and F5) with octane as reductant. Here, an average ratio of 1:1 between reduced NO_x and formed CO_2 is assumed. The impregnated sample shows the highest total formation of CO_2, reaching 1300 ppm around 400 °C. The SG5 sample demonstrates slightly lower CO_2 formation of about 1200 ppm above 420 °C and higher ignition temperature (Table 2) than the IM5 sample. The ignition temperature is here defined as the temperature for CO_2 formation corresponding to 50% conversion of the hydrocarbon [42,43]. The freeze-dried sol–gel sample shows significantly lower CO_2 formation, with even higher ignition temperature. Analysis of the CO_2 formation over the 2 and 8 wt.% samples (not shown) shows similar trends as for the 5 wt.% samples, i.e. higher CO_2 formation starting at lower temperatures for the impregnated samples than the thermally dried and freeze-dried sol–gel samples, in the corresponding order (SG2 excluded, following the pattern for NO_x conversion, Figs. 2a and 3a). Also the formation of CO_2 increases with the silver loading. Fig. 4b shows the formation of NO_2 vs. temperature over the samples with 5 wt.% nominal silver content, with octane as the reducing agent. The impregnated sample shows high formation of NO_2 above 350 °C. The sol–gel samples, however, show smaller peaks of NO_2 formation in quite narrow temperature intervals: 370–400 °C for the SG5 sample and 370–440 °C for the F5 sample. The maximum formation of NO_2 for the SG5 sample is about 50% lower than for the impregnated sample, and even lower for the F5 sample.

Fig. 5a demonstrates the total CO_2 formation and the CO_2 formation due to combustion, respectively, over the samples containing

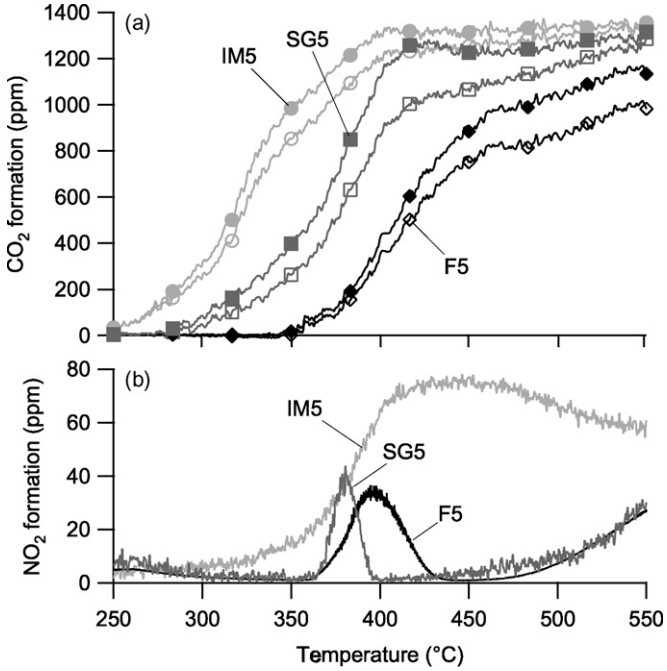

Fig. 4. Formation of (a) CO_2 (filled markers: total CO_2, open markers: CO_2 due to combustion) and (b) NO_2 with octane as reductant for the impregnated (IM5), thermally dried sol–gel (SG5) and freeze-dried sol–gel (F5) samples, with 5 wt.% nominal Ag content. Inlet gas flow composition: 500 ppm NO, 188 ppm C_8H_{18} (1500 ppm HC_1), 5% O_2, Ar bal. GHSV: 30,000 h^{-1}. Temperature measured 15 mm before the monolith sample.

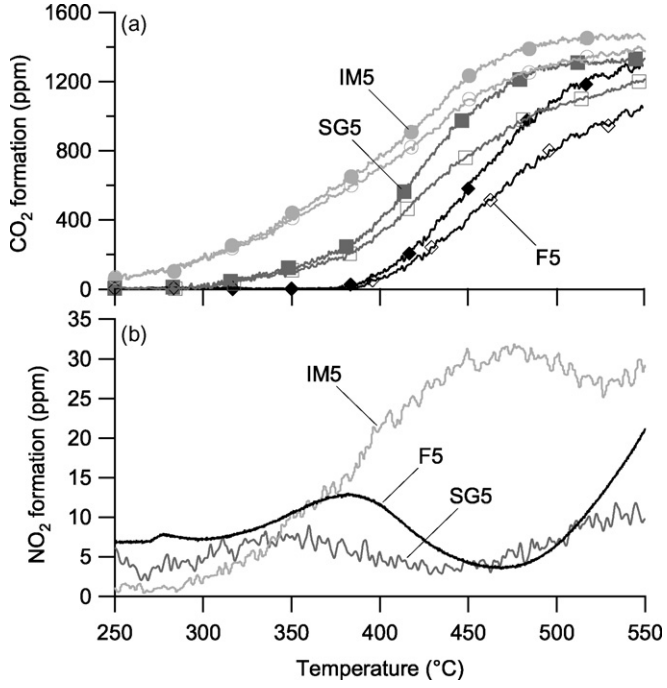

Fig. 5. Formation of (a) CO_2 (filled markers: total CO_2, open markers: CO_2 due to combustion) and (b) NO_2 with propene as reductant for the impregnated (IM5), thermally dried sol–gel (SG5) and freeze-dried sol–gel (F5) samples, with 5 wt.% nominal Ag content. Inlet gas flow composition: 500 ppm NO, 500 ppm C_3H_6 (1500 ppm HC_1), 5% O_2, Ar bal. GHSV: 30,000 h^{-1}. Temperature measured 15 mm before the monolith sample.

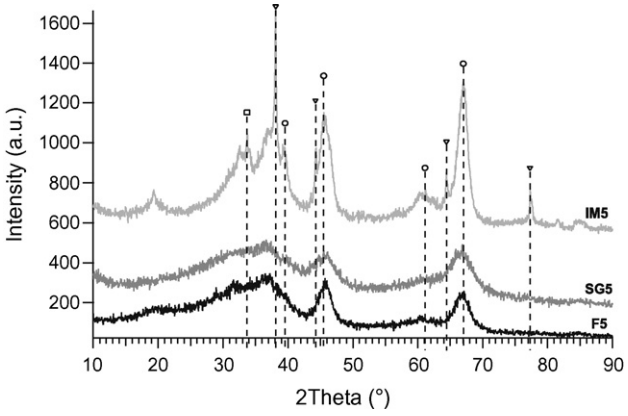

Fig. 6. X-ray diffraction patterns for the impregnated (IM5), sol–gel (SG5) and freeze-dried sol–gel (F5) samples, with 5 wt.% nominal silver content. Peak assignments from She and Flytzani-Stephanopoulos [25] and the ICDD PDF-4+ database [44]. Triangles: Ag^0; circles: Al_2O_3; squares: $AgAlO_2$.

5 wt.% nominal silver loading and with propene as the reducing agent. The trend is similar as for octane as reductant, although the CO_2 formation increases for all samples. The ignition temperature is also higher for all samples, compared to octane. The maximum CO_2 formation over the F5 sample is almost similar as for the SG5 sample. Fig. 5b shows the NO_2 formation for the selected samples with propene as reductant. All samples follow similar trends as for octane, albeit the amount of formed NO_2 is significantly lower and the peaks in NO_2 formation are less pronounced.

3.2. Characterization

3.2.1. N_2 sorption

As can be seen in Table 3, all samples display relatively high specific surface area within the range of $183 \pm 30\ m^2/g$. In comparison, the sol–gel samples show very narrow pore-size distribution, especially the freeze-dried samples. The mean pore diameter is also quite low for these samples, between 30 and 40 Å. The impregnated samples show a much wider pore-size distribution (with the exception of IM5), with a mean pore diameter of 100–120 Å.

3.2.2. XRD

Fig. 6 shows the XRD patterns for the three samples with a nominal Ag content of 5 wt.%, prepared by the routes presented in Fig. 1. The impregnated sample shows clear diffraction peaks assigned to metallic silver and to silver aluminate ($AgAlO_2$ [15,25] or xAg_2O–Al_2O_3 [44]). None of these peaks assigned to silver containing compounds can be observed for the sol–gel samples, except for a subtle indication of the presence of silver species by the diffuse peak between $2\theta = 30$–40°. The absence of clear diffraction peaks (except for alumina) in the spectra of the sol–gel samples indicates amorphous silver or very small silver particles. From the broadening and intensity of the peaks for the different samples it can be concluded that the particle size is likely several times smaller in the sol–gel samples than in the impregnated sample.

3.2.3. XPS

The results from the XPS measurements of the samples with 5% nominal silver content after pre-oxidation and pre-reduction, respectively, are shown in Fig. 7 and Table 4. All samples show a shift in the binding energy (BE) of the Ag $3d_{5/2}$ peak towards lower BE, compared to metallic silver (BE = 368.3 eV), indicating higher oxidation state [45–47]. After pre-oxidation, the impregnated and thermally dried sol–gel samples ($IM5_{ox}$ and $SG5_{ox}$) show BE = 367.7 eV, while the freeze-dried sol–gel ($F5_{ox}$) shows BE = 367.4 eV. The pre-reduced samples (indexed "red") all show

Table 3
Specific surface area, pore-size distribution and silver content of the prepared samples.

Sample	Specific surface area[a] (m^2/g)	Pore-size distribution[a] (Å)	Mean pore diameter[a] (Å)	Nominal Ag content (wt.%)
SG2	169	20–100	43	2
SG5	197	20–77	30	5
SG8	186	20–86	40	8
F2	213	20–60	30	2
F5	188	20–80	30	5
F8	179	20–60	30	8
IM2	157	20–220	120	2
IM5	177	50–130	100	5
IM8	155	40–190	120	8

[a] Powder samples before coating onto monoliths. Instrument lower measuring limit for pore diameter is 20 Å.

Table 4
Binding energies for Ag $3d_{5/2}$ and C 1s orbitals (eV).

	Schön [45]	Bielmann et al. [46]	Weaver and Hoflund [47]	Moulder et al. [35]
Ag^0	368.1 ± 0.1	368.0	368.0	368.1–368.3
Ag_2O	367.7 ± 0.2	367.6	367.7	367.8–368.4
AgO	367.4 ± 0.2	367.2	367.3	367.4–368.0
C 1s	284.6 ± 0.1	–	284.2	284.5

This work[a]	Ag $3d_{5/2}$		C 1s
	Ox	Red	
IM5	367.8	367.5	284.5
SG5	367.7	367.3	284.5
F5	367.5	367.5	284.5

[a] Spectra shifted against C 1s (284.5 eV [35]) due to charging of the material.

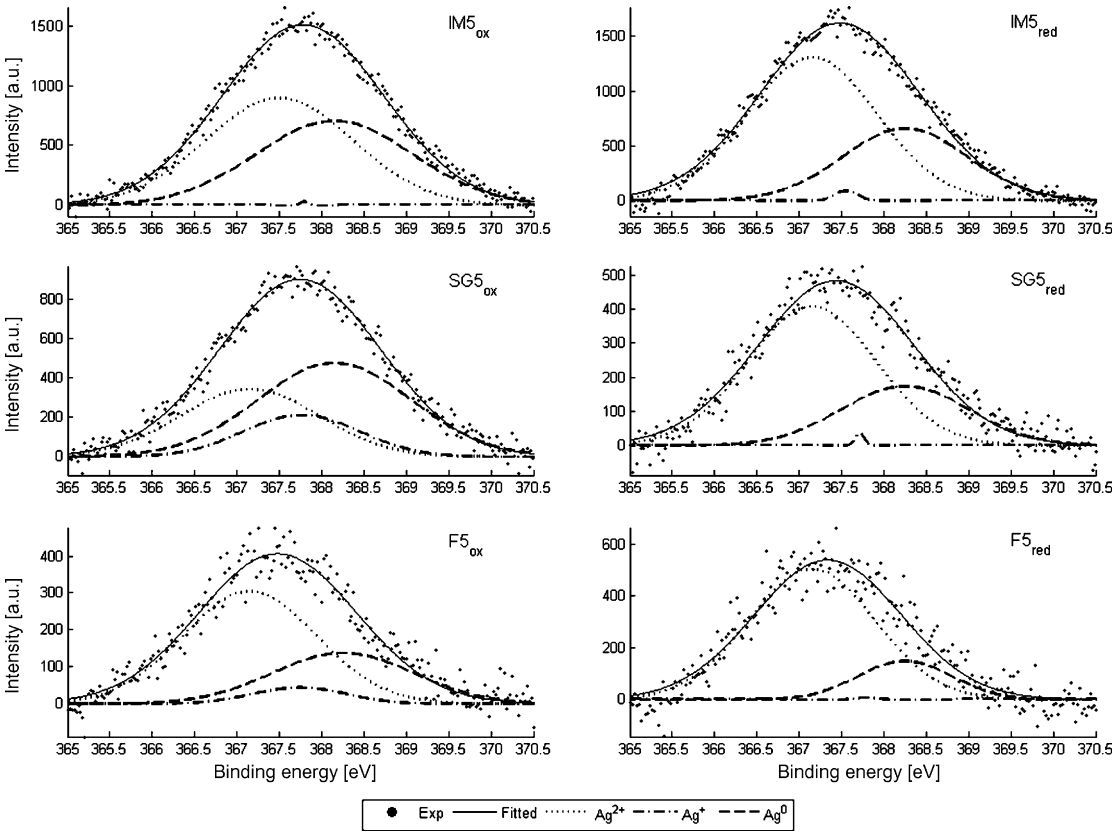

Fig. 7. XPS spectra for the IM5, SG5 and F5 samples. The samples were pre-treated in 5% O_2 (ox, left) or 4% H_2 (red, right) at 400 °C for 10 min and then cooled below 100 °C in the same gas composition. Total gas flow: 300 ml/min, Ar bal. Experimental values are shown by dots; the fitted Gaussian peak is shown by a line. Deconvolution peaks: Ag^{2+} (dotted line), Ag^+ (dash-dotted line) and Ag^0 (dashed line).

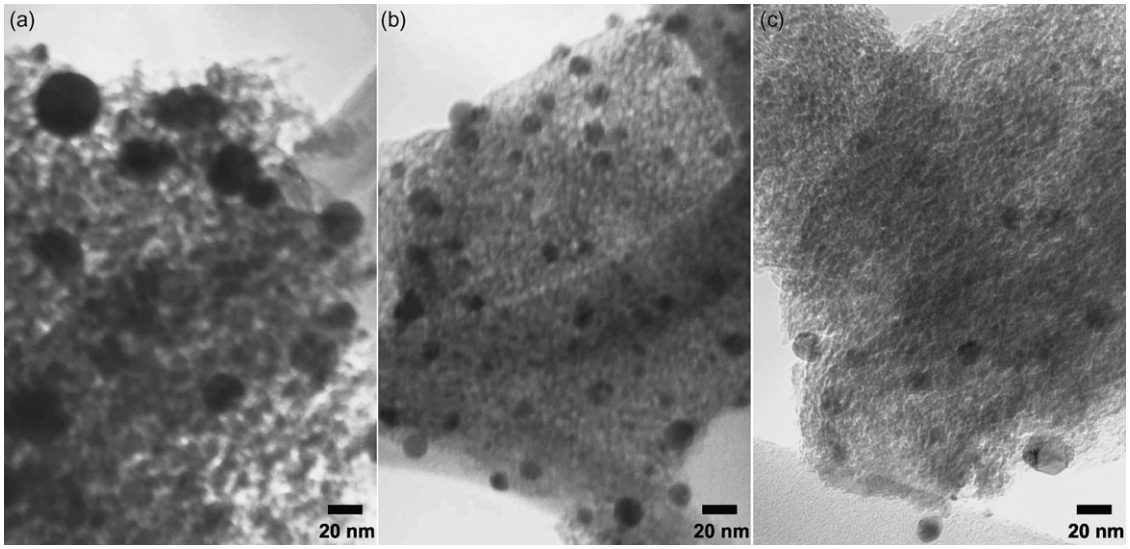

Fig. 8. TEM micrographs of the IM5 (a), SG5 (b) and F5 (c) samples.

BE = 367.4 eV, actually a more oxidized state of silver than for the pre-oxidized samples (except for $F5_{ox}$). The deconvolutions of the peaks confirm these observations, showing a higher proportion of Ag^{2+} for the $IM5_{red}$ and $SG5_{red}$ samples than for the $IM5_{ox}$ and $SG5_{ox}$ samples, while the F5 sample is not influenced by the pre-treatment to the same extent. These results will be discussed further in this article.

3.2.4. TEM

Fig. 8 shows TEM micrographs of the SG5, F5 and IM5 samples. The images clearly show that the silver is less dispersed in the IM5 sample than in either of the sol–gel samples. The silver particles are quite large in the impregnated sample, around 20 nm in diameter, compared to the sol–gel samples where the particles generally are below 10 nm in diameter. The difference between the two sol–gel samples (the SG5 and F5 samples) is not as obvious, although it seems as the SG5 sample contains a larger number of silver particles visible in the micrograph.

3.2.5. Surface acidity

The nature of the surface OH-groups were investigated for some of the samples using the background spectra obtained by DRIFTS (not shown). In the background spectra several peaks appear in the 3800–3650 cm^{-1} range, which are owing to OH stretching vibrations [48]. The peak distribution is similar for all samples investigated.

3.3. Discussion

3.3.1. Dispersion and chemical state of silver

Metallic silver supported on alumina is active for the combustion of hydrocarbons and oxidation of NO to NO_2 [4,8,14,20,23,25,30], whereas oxidized silver, present in the form of e.g. silver ions, silver aluminate or oxides, is shown to promote the formation of N_2 during HC-SCR conditions [14,20,23,25,30,49]. Furthermore, silver ions and small silver clusters have been suggested to act as dopants, activating the alumina matrix for NO_2 adsorption [27]. Small silver clusters ($Ag_n^{\delta+}$) have also been suggested as the active site for HC-SCR [26,28,29] and have e.g. been shown to activate the reductant by partial oxidation and also promote the formation of surface nitrate species [26]. This implies that samples active for NO_x reduction most likely contain silver in an oxidized/ionic state and/or as $Ag_n^{\delta+}$ clusters, very finely distributed throughout the alumina matrix.

The XRD patterns (Fig. 6) reveal the presence of metallic silver in the impregnated sample. As no peaks assigned to metallic silver can be observed for the sol–gel samples, the silver is likely well distributed throughout the alumina matrix. This is also supported by the TEM micrographs (Fig. 8), showing more dispersed silver in the sol–gel samples. The XPS spectra (Fig. 7) show that all samples contain silver in a more or less oxidized state at the sample surface, even though the peaks are broad and the shifts are small. The results for the impregnated (IM5) and thermally dried sol–gel (SG5) samples are peculiar, as the pre-reduced samples show a lower BE, i.e. higher oxidation state of silver than the pre-oxidized samples. This may be explained by the findings of Guo et al. [50], who have shown that for small silver clusters on an Al_2O_3 surface, the Ag 3d peaks shift toward higher BE when exposed to oxygen, especially at elevated temperatures. There may exist small silver clusters on the sample surface of the IM5 and SG5 samples, causing a shift towards higher binding energies during oxidation, even though most part of the surface silver species are in an oxidized state compared to metallic silver, i.e. integrated with the alumina matrix. This is easily imagined for the impregnated sample, as the silver precursor is dispersed on the surface of the support during preparation of the sample and also considering the presence of metallic silver in the sample. However there is also a possibility that this is valid for the SG5 sample: such small silver clusters would not show any X-ray diffraction patterns. The stability of the freeze-dried sol–gel sample (F5) may be attributed to that the silver is more integrated in the alumina matrix, leaving no silver clusters at the sample surface able to cause this shift.

Together, the results from the TEM, XRD and XPS analyses suggest that the sol–gel samples contain more non-metallic silver, as clusters and/or oxidized silver species, which are more finely dispersed throughout the alumina matrix compared to the impregnated sample. The XPS results also indicate that the freeze-dried sol–gel method results in more dispersed silver than the thermally dried sol–gel, leaving no silver clusters at the sample surface.

Concerning the impact of the preparation method for the accessibility of the silver species, it is clear that preparation via sol–gel, in contrast to impregnation, will embed some of the silver species into the alumina matrix. However, due to the porous structure of the sol–gel prepared samples, a high ratio of the silver species should be accessible. Also, this porous structure is favourable for long-range activation of the alumina matrix, proposed by Hellman and Grönbeck [27], which allows embedded silver species to be active in

parts of the HC-SCR reaction. Preparation via impregnation results in silver distributed only on the surface of the support, theoretically giving access to all silver deposited on the alumina. However, agglomeration of silver species forming metallic silver reduces the ratio of accessible silver, as the bulk silver does not take part in the HC-SCR reaction. Further, metallic silver is undesired as it promotes the combustion of the reductant, as mentioned above.

3.3.2. Surface acidity

Since the surface acidity is an important factor for the HC-SCR reaction, the surface OH-groups in the samples were characterized using DRIFT spectroscopy in accordance with Ingelsten et al. [51]. Knözinger and Ratnasamy [48] have proposed a model where five different types of surface OH-groups are coordinated to tetrahedral and/or octahedral aluminium ions, which gives rise to different vibrational frequencies. The OH configurations possess different properties as a consequence of their different net charges, and one property that is influenced is the acidity. Our evaluation shows a distribution of peaks in the OH stretching region, which is similar for all samples. The OH distribution coincides with the results of Knözinger and Ratnasamy, and thus we conclude that the surface acidity is similar for the samples included in this study. The surface acidity will hence not be the cause for the differences in catalytic performance observed for the different samples.

3.3.3. Octane as reducing agent

The SCR reaction over $Ag–Al_2O_3$ catalysts is most likely dependent on two factors: the ability to reduce NO_x to N_2 and to activate (partially oxidize) the reducing agent, i.e. the hydrocarbon. In a recent study [26], Shimizu et al. reported the role of $Ag_n^{\delta+}$ clusters as together with hydrogen activating molecular O_2 to superoxide ions during H_2 assisted propane-SCR, subsequently activating the hydrocarbon reductant. It is reasonable to assume a similar role, i.e. activating the reductant, for these $Ag_n^{\delta+}$ clusters during HC-SCR without hydrogen. In another study [12], Shimizu et al. reported that partially oxidized hydrocarbon (carbonate and carboxylate) species on the catalyst surface suppress the NO_x reduction during *n*-octane-SCR over a 2 wt.% $Ag–Al_2O_3$ catalyst. By addition of water to the feed such species are removed from the surface, which results in increased NO_x reduction. As the flow reactor experiments in the present study were performed in the absence of water, the prevailing conditions most likely promote the formation of carbonaceous surface species.

A comparison of the NO_x reduction profiles of the samples with 5 wt.% nominal silver loading (Fig. 3b) strongly suggests that the preparation method is important for the NO_x reduction. According to the XRD results (Fig. 6) the impregnated sample contains metallic silver, but also silver clusters according to the XPS results (Fig. 7). Fig. 4a show that most CO_2 formation over the impregnated sample is due to combustion of the reductant. This may explain both the low NO_x reduction for the IM5 sample and the low temperature for maximum NO_x reduction. The metallic silver, together with the silver clusters, should be able to activate the octane at low temperatures by partial oxidation. Probably, these silver species also are active for the oxidation of NO to form nitrates [14], increasing the NO_x reduction at low temperatures. The continuous formation of relatively high amounts of gas phase NO_2 over the IM5 sample at higher temperatures (above 350 °C, Fig. 4b) supports this notion. The freeze-dried sol–gel sample shows NO_x reduction at significantly higher temperatures than the impregnated sample. It is likely that the preparation via sol–gel and subsequent freeze-drying promotes dispersed silver throughout the alumina matrix, in contrast to silver concentrated at the surface as in the impregnated sample. Freeze-drying of the gel preserves the pore structure of the sample to a higher degree than thermal drying. This is due to that the high compressing forces over pores with small diameter during evaporation of the water in the gel [52] are avoided by the sublimation of ice. Further, and more importantly, the freeze-drying procedure also prevents agglomeration of silver, as weakly bound silver ions or complexes are fixated by the ice [53], likely minimizing the formation of metallic silver or silver clusters in the samples prepared by freeze-dried sol–gel. This is supported by the results from the XRD, XPS and TEM analyses. Due to the high dispersion of the silver in the F5 sample, the oxidized silver species in the sample should not be readily reduced to clusters by the reductant until high temperatures are reached. The formation of CO_2 due to combustion of the reductant over the F5 sample (Fig. 4a) is significantly lower than over the corresponding impregnated sample. The high temperature for maximum NO_x reduction, the high NO_x reduction (Fig. 3b) and the decrease in NO_2 formation above 430 °C (Fig. 4b) for the freeze-dried sol–gel sample further implies well dispersed non-metallic silver in the sample. The thermally dried sol–gel sample (the SG5 sample) demonstrates the highest NO_x reduction with octane compared to the other samples. The CO_2 formation due to combustion over the SG5 sample is somewhat lower than for the impregnated sample, but higher than for the F5 sample. Also, the peak in NO_2 formation (Fig. 4b) for the SG5 sample is higher than for the F5 sample. According to the XPS results (Fig. 7) silver clusters are present in the SG5 sample, however no metallic silver according to the XRD results (Fig. 6). This is also supported by the higher formation of NO_2 and CO_2 due to combustion over the SG5 sample compared to the F5 sample. Shimizu et al. reported that Ag^+ ions reductively agglomerated to $Ag_n^{\delta+}$ clusters under hydrogen gas flow, which were redispersed to Ag^+ under oxygen flow [26]. This may occur to a lesser extent during HC-SCR, unassisted by hydrogen, thereby forming a higher amount of silver clusters, possibly also larger clusters, in the SG5 sample. Together with the high NO_x reduction of the SG5 sample, these findings suggest that the ratio between silver clusters and oxidized silver species in the catalyst is crucial for a high NO_x reduction. This ratio is dependent on the type of reductant, as different reductants are activated during different conditions, as e.g. temperature. Also, the ability to reduce oxidized silver species to clusters should be dependent on the nature of the reductant.

The samples with 2 wt.% nominal silver loading show a plateau in the NO_x reduction with octane as reducing agent (Fig. 3a), also shown for the F5 sample. According to Shimizu et al. [14] nitrates are dominant surface species at low temperature *n*-hexane-SCR, while surface acetates dominate at high temperatures. It is further proposed that nitrates formed by oxidation of NO are reduced by partially oxidized hydrocarbon species [14]. Since the samples with 2 wt.% nominal silver content in the present study most likely contain low amounts of metallic silver or silver clusters, relatively high temperatures are required to activate the reductant. The activated hydrocarbon may subsequently reduce nitrates, formed on the catalyst surface at lower temperatures [14], shown as a distinct increase in NO_x reduction at about 375 °C. When the surface nitrates are reduced, the SCR reaction may be inhibited by partially oxidized hydrocarbon species poisoning the surface [12], resulting in the plateau in activity seen for these samples. As the temperature increases, the hydrocarbon surface species are further activated and/or oxidized, which enables further reduction of NO_x. The high temperature for maximum NO_x reduction further suggests a high content of oxidized silver in these samples. The SG2 sample shows low NO_x reduction compared to the other samples, although at similar temperatures (Fig. 3a). This may be due to low loading of silver in general for this sample.

The samples with 8 wt.% silver loading generally show low NO_x reduction with octane as reductant (Fig. 3c) mainly due to combustion of the octane, in accordance with the previous discussion. For the impregnated sample (IM8), the NO_x reduction at very low temperatures (~250 °C) is clearly higher than for the

other samples, indicating high metallic silver and silver cluster loading in the impregnated sample. However, the temperature for maximum NO_x reduction (Table 1) is surprisingly high for this sample. One possibility may be that although the sample was stabilized by calcination, the high amount of silver may cause the sample to change during reaction conditions. However, this is not likely as the cooling and heating ramps yielded very similar results in terms of NO_x reduction. Another possibility is that the sample contains much less silver than stated, but this is contradicted by the high activity at low temperatures for both reductants. The maximum NO_x reduction for the freeze-dried sample occurs at a high temperature despite the high silver loading. This indicates that a low amount of metallic silver is present in this sample, which further supports that a high distribution of silver throughout the alumina matrix is obtained by the freeze-dried sol–gel method.

As temperature ramps were used in these experiments, it is important to consider the issue of hystereses between the heating and cooling ramps. Such hystereses were observed (not shown), most prominently for the 2 wt.% samples with octane as reductant, as the plateau in NO_x reduction was not observed for the cooling ramp. This is explained by that the carbonaceous species do not form when approaching the measuring conditions from higher temperatures. Since the temperature ramps used were relatively slow, it is most likely that this hysteresis will be observed also in steady-state experiments, using the appropriate temperature intervals and reaching the measuring conditions both from higher and lower temperatures. Other differences between the heating and cooling ramps than those mentioned above were small and thus we conclude that the hystereses observed do not have any significant impact on the conclusions from this study.

3.3.4. Propene as reductant

The results for propene as reductant generally agree with the results for octane and further coincide with the previous discussion about the preparation methods. The NO_x reduction for the freeze-dried sol–gel samples is in general higher than for *n*-octane as reductant, indicating that propene more readily reduces the oxidized silver species in the samples to silver clusters, however at high temperatures. Increased silver loading generally results in a lower temperature for the maximum NO_x reduction and broader NO_x reduction temperature window, most clearly observed for the freeze-dried sol–gel samples. The formation of CO_2 and NO_2 over the samples with 5 wt.% nominal silver content (Fig. 5) coincides with the results for octane (Fig. 4), but in general the CO_2 formation over the samples is higher for propene as reductant, although at higher temperatures compared to octane. The higher CO_2 formation is according to Fig. 5a due to that even though propene is more difficult to activate than octane, it is more easily combusted at elevated temperatures, in accordance to the previous discussion. The low conversion over the IM5 sample is therefore probably due to combustion of propene, likely also valid for the SG5 sample as larger silver clusters may be formed on the surface of this sample.

The SG8 sample shows high maximum NO_x reduction, however at a surprisingly high temperature. This increase in temperature compared to the SG5 sample indicates less silver clusters in the sample, according to the previous discussion. However, this is contradicted by the decrease in temperature for maximum NO_x reduction between the SG5 and the SG8 sample for octane as reductant (Fig. 3c). This may be due to the different characteristics of the reducing agents. The freeze-dried sol–gel sample (F8) shows similar NO_x reduction as the other samples prepared by this route. However, the temperature corresponding to the maximum NO_x conversion is even lower. This implies the presence of silver clusters at lower temperatures. The high NO_x reduction over all freeze-dried sol–gel samples, with propene as reductant, indicates that the samples contain a high amount of oxidized silver species (i.e. finely dispersed silver) possibly reduced to silver clusters during the SCR reaction by the reductant.

4. Conclusions

A new preparation method for silver-alumina HC-SCR catalysts, via freeze-dried sol–gel is presented. The results from XRD, XPS and TEM analyses show that the catalysts prepared by this method are composed of very small particles with the silver finely distributed throughout the alumina matrix. Flow reactor experiments show high activity for NO_x reduction for all freeze-dried sol–gel samples with propene as reductant, while the activity is lower for octane. The NO_x reduction temperature window is broader and shifted towards lower temperatures when using octane as reductant, compared to propene. This is also generally the case when increasing the silver loading of the samples. Comparisons between samples prepared by different methods, i.e. thermally dried sol–gel and impregnation, were made. The XPS results strongly indicate the presence of silver clusters at the surface of samples prepared by these other techniques, while it is proposed that XPS is a method for detecting silver clusters on the surface of silver alumina catalysts. Together with the flow reactor results, this suggests that the ratio between silver clusters and oxidized silver is crucial to achieve high NO_x reduction by the HC-SCR technique. This ratio is different for propene and octane, while it is suggested to be dependent on the reducing agent used in the SCR reaction. Further, it is proposed that the high activity for the freeze-dried sol–gel samples with propene as reductant is due to a high content of oxidized silver, reduced to silver clusters by the reductant. These properties are most likely due to the preparation method.

Acknowledgements

This work is financially supported by MISTRA (The Foundation for Strategic Environmental Research) and the Swedish Road Administration and has been performed as part of the MISTRA programme E4 (Energy Efficient Reduction of Exhaust Emissions from Vehicles), within the Competence Centre for Catalysis (KCK). KCK is financially supported by Chalmers University of Technology, the Swedish Energy Agency and the member companies: AB Volvo, Volvo Car Corporation, Scania CV AB, GM Powertrain Sweden AB, Haldor Topsoe A/S and The Swedish Space Corporation. Financial support from Knut and Alice Wallenberg Foundation, Dnr KAW 2005.0055, is gratefully acknowledged.

References

[1] IPCC, Climate Change 2007: The Physical Science Basis. Contribution of Working Group I to the Fourth Assessment Report of the Intergovernmental Panel on Climate Change, Cambridge University Press, Cambridge, United Kingdom and New York, NY, USA, 2007.
[2] K. Masuda, K. Tsujimura, K. Shinoda, T. Kato, Appl. Catal. B 8 (1996) 33–40.
[3] N. Aoyama, K. Yoshida, A. Abe, T. Miyadera, Catal. Lett. 43 (1997) 249–253.
[4] K.A. Bethke, H.H. Kung, J. Catal. 172 (1997) 93–102.
[5] T.E. Hoost, R.J. Kudla, K.M. Collins, M.S. Chattha, Appl. Catal. B 13 (1997) 59–67.
[6] T. Miyadera, Appl. Catal. B 13 (1997) 157–165.
[7] H.W. Jen, Catal. Today 42 (1998) 37–44.
[8] T. Miyadera, Appl. Catal. B 2 (1993) 199–205.
[9] T. Miyadera, Appl. Catal. B 16 (1998) 155–164.
[10] S. Kameoka, Y. Ukisu, T. Miyadera, Phys. Chem. Chem. Phys. 2 (2000) 367–372.
[11] A. Keshavaraja, X. She, M. Flytzani-Stephanopoulos, Appl. Catal. B 27 (2000) L1–L9.
[12] K. Shimizu, A. Satsuma, T. Hattori, Appl. Catal. B 25 (2000) 239–247.
[13] Y.B. Yu, H. He, Q.C. Feng, J. Phys. Chem. B 107 (2003) 13090–13092.
[14] K. Shimizu, J. Shibata, H. Yoshida, A. Satsuma, T. Hattori, Appl. Catal. B 30 (2001) 151–162.
[15] T. Nakatsuji, R. Yasukawa, K. Tabata, K. Ueda, M. Niwa, Appl. Catal. B 17 (1998) 333–345.
[16] L.E. Lindfors, K. Eranen, F. Klingstedt, D.Y. Murzin, Top. Catal. 28 (2004) 185–189.
[17] G.K. Boreskov, Catalysis 3 (1982) 39.

[18] S. Satokawa, J. Shibata, K. Shimizu, S. Atsushi, T. Hattori, Appl. Catal. B 42 (2003) 179–186.
[19] R. Burch, J.P. Breen, C.J. Hill, B. Krutzsch, B. Konrad, E. Jobson, L. Cider, K. Eranen, F. Klingstedt, L.E. Lindfors, Top. Catal. 30/31 (2004) 19–25.
[20] F.C. Meunier, J.P. Breen, V. Zuzaniuk, M. Olsson, J.R.H. Ross, J. Catal. 187 (1999) 493–505.
[21] K. Arve, L. Capek, F. Klingstedt, K. Eranen, L.E. Lindfors, D.Y. Murzin, J. Dedecek, Z. Sobalik, B. Wichterlova, Top. Catal. 30/31 (2004) 91–95.
[22] K. Arve, E.A. Popov, M. Ronnholm, F. Klingstedt, J. Eloranta, K. Eranen, D.Y. Murzin, Chem. Eng. Sci. 59 (2004) 5277–5282.
[23] N. Bogdanchikova, F.C. Meunier, M. Avalos-Borja, J.P. Breen, A. Pestryakov, Appl. Catal. B 36 (2002) 287–297.
[24] A. Iglesias-Juez, A.B. Hungria, A. Martinez-Arias, A. Fuerte, M. Fernandez-Garcia, J.A. Anderson, J.C. Conesa, J. Soria, J. Catal. 217 (2003) 310–323.
[25] X. She, M. Flytzani-Stephanopoulos, J. Catal. 237 (2006) 79–93.
[26] K. Shimizu, M. Tsuzuki, K. Kato, S. Yokota, K. Okumura, A. Satsuma, J. Phys. Chem. C 111 (2007) 950–959.
[27] A. Hellman, H. Grönbeck, Phys. Rev. Lett. 100 (2008) 116801.
[28] A. Satsuma, J. Shibata, K. Shimizu, T. Hattori, Catal. Surv. Asia 9 (2005) 75–85.
[29] J. Shibata, K. Shimizu, Y. Takada, A. Shichia, H. Yoshida, S. Satokawa, A. Satsuma, T. Hattori, J. Catal. 227 (2004) 367–374.
[30] A. Iglesias-Juez, M. Fernandez-Garcia, A. Martinez-Arias, Z. Schay, Z. Koppany, A.B. Hungria, A. Fuerte, J.A. Anderson, J.C. Conesa, J. Soria, Top. Catal. 30/31 (2004) 65–70.
[31] E. Seker, J. Cavataio, E. Gulari, P. Lorpongpaiboon, S. Osuwan, Appl. Catal. A 183 (1999) 121–134.
[32] S. Brunauer, P.H. Emmet, E. Teller, J. Am. Chem. Soc. 60 (1938) 309–319.
[33] E.P. Barrett, L.G. Joyner, P.P. Halenda, J. Am. Chem. Soc. 73 (1951) 373–380.
[34] L. Olsson, E. Fridell, J. Catal. 210 (2002) 340–353.
[35] J.F. Moulder, W.F. Stickle, P.E. Sobol, K.D. Bomben, Handbook of X-Ray Photoelectron Spectroscopy, PerkinElmer Corporation - Physical Electronics Division, Eden Prairie, 1992.
[36] H.H. Ingelsten, A. Palmqvist, M. Skoglundh, J. Phys. Chem. B 110 (2006) 18392–18400.
[37] R. Matarrese, H.H. Ingelsten, M. Skoglundh, J. Catal. 258 (2008) 386–392.
[38] J. Dawody, M. Skoglundh, S. Wall, E. Fridell, J. Mol. Catal. A: Chem. 225 (2005) 259–269.
[39] M. Skoglundh, H. Johansson, L. Lowendahl, K. Jansson, L. Dahl, B. Hirschauer, Appl. Catal. B 7 (1996) 299–319.
[40] L. Kylhammar, A. Palmqvist, M. Skoglundh, Top. Catal. 42/43 (2007) 119–122.
[41] P.B. Weiszs, C.D. Prater, Adv. Catal. 6 (1954) 143–196.
[42] J.T. Kummer, Prog. Energy Combust. Sci. 6 (1980) 177–199.
[43] K.C. Taylor, Chem. Tech. 20 (1990) 551–555.
[44] JCPDS - International Centre for Diffraction Data, Philadelphia, USA, 2007.
[45] G. Schön, Acta Chem. Scand. 27 (1973) 2623–2633.
[46] M. Bielmann, P. Schwaller, P. Ruffieux, O. Groning, L. Schlapbach, P. Groning, Phys. Rev. B 65 (2002) 235431.
[47] J.F. Weaver, G.B. Hoflund, J. Phys. Chem. 98 (1994) 8519–8524.
[48] H. Knözinger, P. Ratnasamy, Cat. Rev.: Sci. Eng. 17 (1978) 31–70.
[49] P. Sazama, L. Capek, H. Drobna, Z. Sobalik, J. Dedecek, K. Arve, B. Wichterlova, J. Catal. 232 (2005) 302–317.
[50] D. Guo, Q. Guo, K. Zheng, E.G. Wang, X. Bao, J. Phys. Chem. C 111 (2007) 3981–3985.
[51] H.H. Ingelsten, A. Hildesson, E. Fridell, M. Skoglundh, J. Mol. Catal. A: Chem. 209 (2004) 199–207.
[52] R.K. Iler, The Chemistry of Silica, John Wiley & Sons, 1979, pp. 528–539.
[53] D.W. Johnson Jr., P.K. Gallagher, F.J. Scnettler, E.M. Vogel, Ceram. Bull. 56 (1977) 785–788, 792.